HHS Public Access

Author manuscript

Cancer Lett. Author manuscript; available in PMC 2017 September 28.

Published in final edited form as:

Cancer Lett. 2016 September 28; 380(1): 69–77. doi:10.1016/j.canlet.2016.06.003.

Developing Oxygen-Enhanced Magnetic Resonance Imaging as a Prognostic Biomarker of Radiation Response*

Derek A. White, PhD[a,b], **Zhang Zhang, PhD**[c], **Li Li, MD**[a], **Jeni Gerberich, BS**[a], **Strahinja Stojadinovic, PhD**[c], **Peter Peschke, PhD**[d], and **Ralph P. Mason, PhD**[a,§]

[a]Department of Radiology, UT Southwestern Medical Center, Dallas, Texas 75235 USA

[b]Department of Bioengineering, University of Texas at Arlington, Arlington, Texas 76019 USA

[c]Department of Radiation Oncology, UT Southwestern Medical Center, Dallas, Texas 75235 USA

[d]German Cancer Center, Heidelberg, Germany

Abstract

Oxygen-Enhanced Magnetic Resonance Imaging (OE-MRI) techniques were evaluated as potential non-invasive predictive biomarkers of radiation response. Semi quantitative blood-oxygen level dependent (BOLD) and tissue oxygen level dependent (TOLD) contrast, and quantitative responses of relaxation rates (ΔR_1 and ΔR_2*) to an oxygen breathing challenge during hypofractionated radiotherapy were applied. OE-MRI was performed on subcutaneous Dunning R3327-AT1 rat prostate tumors (*n = 25*) at 4.7 T prior to each irradiation (2Fx15 Gy) to the gross tumor volume. Response to radiation, while inhaling air or oxygen, was assessed by tumor growth delay measured up to four times the initial irradiated tumor volume (VQT). Radiation-induced hypoxia changes were confirmed using a double hypoxia marker assay. Inhaling oxygen during hypofractionated radiotherapy significantly improved radiation response. A correlation was observed between the difference in the 2nd and 1st ΔR_1 ($\Delta\Delta R_1$) and VQT for air breathing rats. The TOLD response before the 2nd fraction showed a moderate correlation with VQT for oxygen breathing rats. The correlations indicate useful prognostic factors to predict tumor response to hypofractionation and could readily be applied for patient stratification and personalized radiotherapy treatment planning.

Keywords

stereotactic body radiation therapy (SBRT); Magnetic Resonance Imaging; hypoxia; oxygen; radiation response; reoxygenation

*Presented in part at 23rd Annual meeting of *ISMRM*, Toronto, Canada, June 2015, 57th Annual meeting AAPM, Anaheim CA, July 2015 and 61st Annual Meeting Radiation Research Society, Weston, FL, September, 2015.

§Corresponding author: Ralph P. Mason, PhD, Department of Radiology, UT Southwestern Medical Center, 5323 Harry Hines Blvd., Dallas, TX 75390-9058, Phone: (214) 648-8926, Ralph.Mason@UTSouthwestern.edu.

The authors have no conflicts of interest to disclose.

1. Introduction

Hypoxia is increasingly recognized to play a fundamental role in aggressiveness and therapeutic resistance in many tumors including prostate [1–5]. Hypoxia has been associated with radioresistance in cells [6], pre-clinical animal studies [7–12] and human patients [3, 5, 13]. However, the meta-analysis of Overgaard *et al.* [14] indicated that interventions to overcome hypoxia provided only marginal benefit and it was concluded that the lack of efficacy was likely related to the inability to identify which patients would benefit. Consequently, there is a substantial effort to develop non-invasive measurements of the dynamics of tumor oxygenation, as potential biomarkers for patient stratification [2, 15, 16].

Robust evidence for hypoxia in human tumors has been established at multiple disease sites using the Eppendorf Histograph electrode system [1, 4, 5, 17–20]. This has also been applied extensively in pre-clinical studies, but is highly invasive, technically challenging and no longer commercially available. Analogous measurements of tumor pO_2 and hypoxic fractions have been achieved by direct intra tumoral administration of reporter molecules for ^{19}F [8, 9, 21] and ^{1}H MRI [22], and ESR [11, 23, 24]. These have the distinct benefit of allowing dynamic response to interventions to be assessed non-invasively [8, 9, 11, 22–25]. To avoid violating tumor integrity, reporter molecules may also be delivered intravenously [10, 26], but such measurements invariably bias results towards better perfused and likely less hypoxic regions. The need for reporter molecules complicates potential translation to the clinic.

Hypoxia may be directly observed using nuclear medicine reporters, typically, ^{18}F labeled nitroimidazoles [15, 16, 27], but the associated radioactivity makes them expensive and assessment of dynamic modulation of hypoxia is generally not practical. Analogous use of immunochemistry of nitroimidazole trapping has allowed pulse chase evaluation of hypoxia modulation, but requires biopsy [28].

Oxygen enhanced MRI has been suggested as a potential alternative approach, since it is entirely non-invasive and can be readily added to routine clinical MRI, which is increasingly applied to radiation planning and execution [29]. The tissue water proton apparent transverse relaxation rate (R_2*) is strongly influenced by the concentration of deoxyhemoglobin, which is paramagnetic [2, 28]. This provides blood oxygen level dependent (BOLD) contrast, which is the basis of fMRI used in studies of neuronal activation. R_2* is influenced by conversion of deoxy- to oxyhemoglobin, but is also subject to alteration in flow, hematocrit, and vascular volume, as described by the so-called FLOOD effect [30]. Meanwhile, the spin lattice relaxation rate (R_1) is directly sensitive to the concentration of free oxygen molecules and hence pO_2. This is the basis of tissue oxygen level dependent (TOLD) contrast [31]. Several investigations have examined correlations between BOLD and TOLD based on semi quantitative changes in signal intensity or quantitative relaxation maps. Notably, studies in human tumor xenografts in mice [32], as well as syngeneic tumors in rats [33, 34] and rabbits [35]. The two approaches have also been assessed in humans including volunteer patients [36–38].

Several studies have examined correlations of BOLD with invasive oximetry in pre-clinical studies based on polarographic oxygen electrodes, fluorescent quenched fiber optic probes and ^{19}F MRI [39–41]. Sometimes a strong direct correlation has been observed, while other studies indicated nonlinear correlative trends. Notably, a large BOLD response to a hyperoxic gas breathing challenge was associated with elimination of hypoxia in 13762NF rat breast tumors [41]. A recent report indicated that syngeneic rat prostate tumors could be stratified in terms of radiation response based on TOLD MRI responses to an oxygen breathing challenge before a single dose of radiotherapy [33].

New hypofractionated treatment approaches are gaining popularity for several reasons: i) fewer treatment sessions are convenient to patients and physicians; ii) precise treatment plans may be developed for each irradiation; iii) recent clinical trials are showing enhanced outcome [42]. However, it is thought that radiation response is more influenced by hypoxia, especially when large single- or multi-fraction dose regimens typical of stereotactic body radiotherapy (SBRT) are implemented, since tumor reoxygenation is minor compared to traditional conventional fractionated radiation therapy (CFRT) [43].

Noting the importance of hypoxia and desire for a robust non–invasive approach to assess tumor hypoxia and oxygen dynamics, prompted us to explore OE-MRI with respect to a hypofractionated radiation regimen.

2. Materials and Methods

Investigations were approved by the Institutional Animal Care and Use Committee. The experimental timeline for separate groups of tumors is shown in Table 1. Additional experimental details are provided in Supplementary Materials.

Dunning R3327-AT1 prostate tumors were surgically implanted subcutaneously in the flank of 25 adult male syngeneic Copenhagen rats [9]. The AT1 is a well-characterized anaplastic prostate tumor often used for radiobiological studies [9, 21, 33, 44–46]. Tumors were used for OE-MRI around 19 days after implantation, when they reached a size in the range 0.7–2.1 cm^3. Animals were divided into four groups: unirradiated “Control” (Group 1, $n = 4$), irradiated while inhaling “Air” (Group 2, $n = 9$), irradiated while inhaling “Oxygen” (Group 3, $n = 9$) and immunohistological correlates (Group 4, $n = 3$).

2.1 Oxygen-Enhanced Magnetic Resonance Imaging

Anesthetized rats were provided with a warming pad to maintain body temperature, placed in a 4.7 T MR scanner and physiological parameters recorded using an MR-compatible monitoring and gating system. Baseline R_1 measurements of the tissue water proton signal were obtained with a 2-D multi-slice spin-echo (SEMS) sequence, while the animals breathed air (1 dm^3/min with 1.5–2.0% isoflurane) and at the end of the oxygen breathing challenge. Interleaved dynamic blood-oxygenation level dependent (BOLD or R_2*) and tissue-oxygenation level dependent (TOLD or T_1-weighted) measurements were performed for about 10 minutes for baseline air and during a hyperoxic oxygen breathing challenge (1 dm^3/min O_2 up to 10 minutes). BOLD acquisition used a 2-D multi-slice spoiled gradient-echo with multi-echo (MGEMS) sequence.

2.2 Radiation Therapy

Tumors were irradiated about 24 hrs after OE-MRI experiments. Prior to, and during radiotherapy, the anesthetized animals inhaled either Air (Group 2, $n = 9$) or Oxygen (Group 3, $n = 9$) for at least 15 minutes. Unirradiated tumors ($n = 4$) provided controls. Radiation was applied to the gross tumor volume (GTV) with orthovoltage x-rays at 15 Gy using image-guided radiation therapy with a small animal x-ray irradiator. OE-MRI and irradiation were repeated one week later. Tumor growth was measured weekly until tumors reached 10% body weight or 90 days to assess the response to radiation. Tumor growth delay was determined by the time required for the tumors to reach two (volume doubling time, VDT) and four times (volume quadrupling time, VQT) the initial irradiated tumor volume using simple linear interpolation. Three additional tumors (Group 4) were examined to assess reoxygenation after the first fraction based on immunohistochemistry.

2.3 Immunohistochemistry

A double hypoxia marker approach [28, 47] was used to verify tumor reoxygenation. Immediately after OE-MRI, three tumor bearing rats, while breathing oxygen, were injected intravenously with pimonidazole as a baseline tumor hypoxia marker. About 24 hours later two of the tumors were irradiated with 15 Gy, while the animal was breathing oxygen. The third tumor served as a control. Three days later a second tumor hypoxia marker, CCI-103F, was injected intraperitoneally, while the rats were breathing oxygen. Two hours later, the rats were sacrificed and tumor tissue harvested.

2.4 OE-MRI Data Processing and Analysis

Using in-house algorithms developed in Matlab, voxel-by-voxel %ΔSI in BOLD and TOLD responses with respect to inhaling oxygen were calculated from the whole tumor region-of-interest. BOLD images were selected at a single echo time (TE=20 ms) for analysis. Voxel-by-voxel R_2* maps were generated from BOLD images by fitting the multi-echo data to the echo time (TE) in a nonlinear least squares equation and quantitative ΔR_2* values were calculated. Likewise, R_1 with respect to the repetition times (TR). A log-rank test Kaplan-Meier analysis was used to compare tumor growth for Air, Oxygen and Control groups.

3. Results

3.1 Oxygen-Enhanced Magnetic Resonance Imaging

Tumors showed considerable heterogeneity in terms of baseline R_2* and R_1, as well as responses to oxygen challenge (semi quantitative BOLD and TOLD; quantitative ΔR_2* and ΔR_1; Fig. 1). Mean R_1 for individual tumors ranged from 0.3367 to 0.7122 s^{-1} with a population mean 0.499±0.0259 s^{-1}. Baseline ΔR_1 ranged from −0.006 to 0.12 s^{-1} with a mean 0.041±0.008 s^{-1} for the 18 tumors (Groups 2 and 3; Table 1). Mean R_2* ranged from 27.4 to 69.9 s^{-1} with a mean 51.7±3.1 s^{-1} and ΔR_2* ranged from −3.5 to 9.1 s^{-1} (mean 0.55±0.75 s^{-1}). There were no significant differences between Groups before irradiation, but there was a significant difference in ΔR_2* between Air and Oxygen breathing groups ($P<0.03$) one week after 15 Gy (before the 2nd irradiation). The semi quantitative parameters showed a significant correlation between mean TOLD and BOLD responses for individual

tumors before the 1st irradiation (R>0.6, P<0.005) and before the 2nd irradiation (R>0.6, P=0.0051).

3.2 Radiation Response

Non-irradiated tumors showed a typical VDT = 6.5±0.3 days and VQT = 13±0.4 days with exponential growth up to time of sacrifice at 10% body weight (Fig. 2). All tumors responded to 2×15 Gy with a growth delay regardless of inhaling air or oxygen (Fig. 2A). Tumors growing on animals breathing O_2 tended to express a greater growth delay than tumors in the Air Group (Fig. 2), which was significant for VDT (P<0.001) and VQT (P<0.04) (Table 1, Fig. 2B) and confirmed by the log rank test (Fig. 2C).

Potential correlates of VDT and VQT with OE-MRI were examined (Table 1 and Supplementary Table S1). Moderate correlations were seen for pre irradiation ΔR_1 for both Air and O_2-breathing groups in addition to ΔR_2* for Air and O_2-breathing groups combined (data not shown). The strongest correlation was observed in Group 2 (Air) for change in ΔR_1 response to O_2 challenge between the first and second measurements ($\Delta\Delta R_1$). Those tumors showing the greatest increase in ΔR_1 and had the longest VQT (R>0.9, P<0.002, Fig. 3A). For Group 3, but not for Group 2, there was a modest correlation between TOLD before the 2nd irradiation and VQT (R>0.6, P<0.04, Fig. 3B). Mean BOLD and TOLD responses did not change significantly between fractions (Fig. 4, Table 1), but the fraction of voxels within the tumors showing a TOLD response to O_2 challenge increased significantly (Fig. 4). The BOLD response appeared largely unchanged. These data are consistent with reoxygenation revealed by pulse chase immunohistochemistry (Fig. 5). Extensive hypoxia was observed pre irradiation, which appeared consistent 3 days later in the absence of radiation (HF_{pimo} =28%, $HF_{CCI\text{-}103F}$ =27%; Fig. 5). Irradiated tumors showed significant decrease in hypoxic fraction after 72 hours (HF_{pimo} =9.7%, $HF_{CCI\text{-}103F}$ =0.3%).

4. Discussion

Both, the tumor oxygenation status as well as its treatment-related variation have profound clinical implications, which represent the driving force to further exploit fast and sensitive imaging techniques. OE-MRI is such a non-invasive technology which provides parameters sensitive to changes in tissue oxygenation. Although the idea of altering radiation response based on the simple procedure of breathing hyperoxic gas [8–10, 23, 33, 48] was disappointing when translated to patients, there is a general consensus that lack of success was mainly due to inability to identify those patients who would benefit. This study serves to further assess the potential prognostic utility of OE-MRI [49]. Hypofractionation of Dunning prostate R3327-AT1 tumors was selected as a model system due to evidence of a prompt oxygen response following the application of large radiation doses [50]. We chose one week between two radiation doses to match ongoing clinical trials of hypofractionated SBRT in lung cancer (3×16 Gy over 1½ to 2 weeks [51])

As expected, a significant tumor growth delay was observed and rats breathing oxygen during irradiation showed a greater response (VDT and VQT, Table 1, Fig. 2). However, each cohort exhibited a range of growth delays with overlap between the Air and Oxygen Groups. It was previously reported that tumor growth delay in response to a single dose of

30 Gy, while breathing oxygen was related to pre irradiation TOLD response to an oxygen breathing challenge [33]. A significantly greater VQT was observed for those tumors with large TOLD. Here, we observed a strong correlation between TOLD prior to the 2nd irradiation and VQT for Group 3 (but not Group 2, Fig. 3B). The strongest correlation was observed between VQT and the change in TOLD response ($\Delta\Delta R_1$: baseline vs. 1 week later) for the Air Group (Fig. 3A). Those tumors with increased response to oxygen breathing (positive $\Delta\Delta R_1$) showed a greater tumor growth delay than those showing a reduced response ($P<0.005$). The observed R_1 and R_2* (Fig. 1) are not dissimilar from previous reports for this tumor type at 4.7 T [33, 34]. Present results ($\Delta R_1 = -0.006$ to $0.121\ s^{-1}$) are also comparable to reports of orthotopic gliomas implanted in mice [52], though overall population mean response was somewhat higher (0.04 vs. $0.01\ s^{-1}$ with oxygen or carbogen) than reported for the orthotopic gliomas or squamous cell carcinomas with respect to hyperbaric oxygen [31].

Most parameters showed little change after irradiation, but ΔR_2* response to breathing oxygen was significantly different for Group 3 versus Group 2, one week after 15 Gy irradiation (Table 1). The more negative ΔR_2* is consistent with greater conversion of deoxy- to oxyhemoglobin in response to O_2-breathing challenge and hence improved tumor oxygenation. By contrast Lin *et al.* [53] examined BOLD response of TRAMP-C1 tumors 6 days after 15 Gy and found significantly smaller response compared to controls implying hypoxiation. It was previously reported that only a sub-group of AT1 tumors benefited from oxygen breathing during a single dose of radiation (30 Gy) and these were characterized by larger ΔR_1 [33]. Here, for the split dose (2×15 Gy), O_2-breathing enhanced radiation response, but in terms of OE-MRI parameters, there was a general trend rather than a stratifiable difference in response. However, for the Air–breathing group those with improved oxygenation (positive $\Delta\Delta R_1$), did as well as those with oxygen breathing, whereas those with negative $\Delta\Delta R_1$ did significantly less well. Noting the reported relaxivity of oxygen in tissue at 4.7 T ($r_1 = 9\ *10–4\ Torr^{-1}.s^{-1}$ [52]) the observed changes ($\Delta R_1 = -0.006$ to 0.121) would correspond with $\Delta pO_2 = -6$ to +134 Torr in response to oxygen breathing challenge and $\Delta\Delta R_1 \pm 0.05\ s^{-1}$ implies $\Delta\Delta pO_2 = 55$ Torr suggesting that the observed changes in oxygenation would cause distinct differences in radiation response.

Assessing tumor oxygenation using endogenous contrast based on tissue blood and water is appealing, but there is a potential caveat particularly in terms of BOLD responses. These are predicated on conversion of deoxy- to oxyhemoglobin. Historically, there are reports that hematocrit may decrease in patients during a course of radiation therapy. This is expected to be less of an issue with modern conformal targeting capabilities. Leonard *et al.* recently reported no significant change in the hematocrit of patients undergoing definitive IMRT for prostate cancer [54], though a significant decline, albeit only 1%, was seen in patients receiving hormone ablation therapy. Lower hematocrit would imply smaller BOLD response, but also less capability of delivering oxygen, and thus any reduced BOLD response would actually reflect weaker modulation. Noting that TOLD is primarily sensitive to pO_2 rather than hemoglobin status, again emphasizes why TOLD mat be expected to be a more robust marker of tumor hypoxia and modulation. To further investigate improved oxygenation for Group 3, we applied the pulse chase approach pioneered by van der Kogel *et al.* [47]. The distribution of the bioreductive hypoxia markers pimonidazole and CCI-103F

administered before IR and 3 days after irradiation in the control non-irradiated tumor closely matched, indicating consistent hypoxia. In contrast, irradiated tumors showed significantly decreased marker distribution indicating reduced hypoxia (Fig. 5).

Previous results regarding post irradiation reoxygenation appear contradictory. A significant increase in tumor oxygenation was observed by ^{19}F MRI in Dunning prostate AT1 tumors up to 10 hours after 20 Gy irradiation [50] and by EPR in RIF-1 tumors, 72–120 hours after 20 Gy [24]. Meanwhile, a recent study in FSaII tumors demonstrated secondary cell death, based on clonogenic survival assays 2–5 days, after 20 Gy, attributed to by vascular damage, which was accompanied by a significant increase in hypoxic markers [55]. As levels of hypoxia and response are expected to vary with radiation dose, tumor type, host species and method of anesthesia the need for further investigations is obvious.

OE-MRI is particularly attractive since it is readily translatable to human applications. Several preliminary studies have already shown the use of hyperoxic gas challenge to stimulate BOLD and/or TOLD MRI signal responses in tumors at distinct disease sites (breast [56, 57], cervix [49, 58, 59], brain [38, 60], prostate [61], and liver [62]). Breathing oxygen is particularly appropriate, since this is standard intervention in emergency medicine and thus it is quite straightforward to gain IRB approval. Carbogen ($95\%O_2$, $5\%CO_2$) has been favored by some investigators, but it is reported to cause some respiratory distress and is les swell tolerated. In terms of adding OE-MRI to a routine radiological examination, it would need to be applied before any Gd-contrast agents are applied. As seen in Fig 4, the response to oxygen breathing is quite rapid and therefore do not add an undue burden to the length of radiological exam. Overall the non-invasive nature of the measurements, lack of radioactivity and ease of conducting an oxygen gas challenge make OE-MRI particularly attractive.

In summary, the results further indicate the feasibility of OE-MRI and again suggest that R_1 is more relevant to stratifying tumors than R_2*. Given the non-invasive nature of the measurements and relatively rapid data acquisition, the approach could be rapidly incorporated in future clinical investigations, and should ultimately indicate which patients are likely to benefit from oxygen breathing during irradiation.

Supplementary Material

Refer to Web version on PubMed Central for supplementary material.

Acknowledgments

Supported in part by funds from the National Cancer Institute (5R01 CA139043). MRI experiments were performed in the AIRC, supported by National Institute of Biomedical Imaging and Bioengineering Resource grant (EB015908) and subsidized by NCI Cancer Center Support Grant (1P30 CA142543) and irradiation facilitated by Shared Instrumentation Grant (S10 RR028011). Histology was facilitated by the Imaging Core of the Cancer Center under the guidance of Dr. Kate Phelps. We thank Joshua Gunpat and Rebecca Denney for tumor implantation.

References

1. Menon C, Fraker DL. Tumor oxygenation status as a prognostic marker. Cancer Letters. 2005; 221:225–235. [PubMed: 15808408]

2. Tatum JL, Kelloff GJ, Gillies RJ, Arbeit JM, Brown JM, Chao KSC, Chapman JD, Eckelman WC, Fyles AW, Giaccia AJ, Hill RP, Koch CJ, Krishna MC, Krohn KA, Lewis JS, Mason RP, Melillo G, Padhani AR, Powis G, Rajendran JG, Reba R, Robinson SP, Semenza GL, Swartz HM, Vaupel P, Yang D, Croft B, Hoffman J, Liu GY, Stone H, Sullivan D. Hypoxia: Importance in tumor biology, noninvasive measurement by imaging, and value of its measurement in the management of cancer therapy. Int J Radiat Biol. 2006; 82:699–757. [PubMed: 17118889]

3. Vergis R, Corbishley CM, Norman AR, Bartlett J, Jhavar S, Borre M, Heeboll S, Horwich A, Huddart R, Khoo V, Eeles R, Cooper C, Sydes M, Dearnaley D, Parker C. Intrinsic markers of tumour hypoxia and angiogenesis in localised prostate cancer and outcome of radical treatment: a retrospective analysis of two randomised radiotherapy trials and one surgical cohort study. Lancet Oncology. 2008; 9:342–351. [PubMed: 18343725]

4. Turaka A, Buyyounouski MK, Hanlon AL, Horwitz EM, Greenberg RE, Movsas B. Hypoxic Prostate/Muscle PO_2 Ratio Predicts for Outcome in Patients With Localized Prostate Cancer: Long-Term Results. Int J Radiat Oncol Biol Phys. 2012; 82:E433–E439. [PubMed: 21985947]

5. Milosevic M, Warde P, Menard C, Chung P, Toi A, Ishkanian A, McLean M, Pintilie M, Sykes J, Gospodarowicz M, Catton C, Hill RP, Bristow R. Tumor Hypoxia Predicts Biochemical Failure following Radiotherapy for Clinically Localized Prostate Cancer. Clin Cancer Res. 2012; 18:2108–2114. [PubMed: 22465832]

6. Gray L, Conger A, Ebert M, Hornsey S, Scott O. The concentration of oxygen dissolved in tissues at time of irradiation as a factor in radiotherapy. Br J Radiol. 1953; 26:638–648. [PubMed: 13106296]

7. Rockwell S, Moulder JE. Hypoxic fractions of human tumors xenografted into mice: a review. Int J Radiat Oncol Biol Phys. 1990; 19:197–202. [PubMed: 2143178]

8. Zhao D, Constantinescu A, Chang C-H, Hahn EW, Mason RP. Correlation of Tumor Oxygen Dynamics with Radiation Response of the Dunning Prostate R3327-HI Tumor. Radiat Res. 2003; 159:621–631. [PubMed: 12710873]

9. Bourke VA, Zhao D, Gilio J, Chang C-H, Jiang L, Hahn EW, Mason RP. Correlation of Radiation Response with Tumor Oxygenation in the Dunning Prostate R3327-AT1 Tumor. Int J Radiat Oncol Biol Phys. 2007; 67:1179–1186. [PubMed: 17336219]

10. Elas M, Bell R, Hleihel D, Barth ED, McFaul C, Haney CR, Bielanska J, Pustelny K, Ahn K-H, Pelizzari CA, Kocherginsky M, Halpern HJ. Electron Paramagnetic Resonance Oxygen Image Hypoxic Fraction Plus Radiation Dose Strongly Correlates With Tumor Cure in FSa Fibrosarcomas. Int J Radiat Oncol Biol Phys. 2008; 71:542–549. [PubMed: 18474313]

11. O'Hara JA, Goda F, Demidenko E, Swartz HM. Effect on regrowth delay in a murine tumor of scheduling split-dose irradiation based on direct pO_2 measurements by electron paramagnetic resonance oximetry. Radiat Res. 1998; 150:549–556. [PubMed: 9806597]

12. Schutze C, Bergmann R, Bruchner K, Mosch B, Yaromina A, Zips D, Hessel F, Krause M, Thames H, Kotzerke J, Steinbach J, Baumann M, Beuthien-Baumann B. Effect of F-18 FMISO stratified dose-escalation on local control in FaDu hSCC in nude mice. Radiother Oncol. 2014; 111:81–87. [PubMed: 24636842]

13. Horsman MR, Mortensen LS, Petersen JB, Busk M, Overgaard J. Imaging hypoxia to improve radiotherapy outcome. Nat Rev Clin Oncol. 2012; 9:674–687. [PubMed: 23149893]

14. Overgaard J. Hypoxic radiosensitization: Adored and ignored. J Clin Oncol. 2007; 25:4066–4074. [PubMed: 17827455]

15. Evans SM, Koch CJ. Prognostic significance of tumor oxygenation in humans. Cancer Letters. 2003; 195:1–16. [PubMed: 12767506]

16. Mason RP, Zhao D, Pacheco-Torres J, Cui W, Kodibagkar VD, Gulaka PK, Hao G, Thorpe P, Hahn EW, Peschke P. Multimodality imaging of hypoxia in preclinical settings. QJ Nucl Med Mol Imaging. 2010; 54:259–280.

17. Fyles A, Milosevic M, Pintilie M, Syed A, Levin W, Manchul L, Hill RP. Long-term performance of interstitial fluid pressure and hypoxia as prognostic factors in cervix cancer. Radiother Oncol. 2006; 80:132–137. [PubMed: 16920212]

18. Brizel DM, Sibly GS, Prosmitz LR, Scher RL, Dewhirst MW. Tumor hypoxia adversely affects the prognosis of carcinoma of the head and neck. Int J Radiat Oncol Biol Phys. 1997; 38:285–289. [PubMed: 9226314]

19. Le QT, Chen E, Salim A, Cao HB, Kong CS, Whyte R, Donington J, Cannon W, Wakelee H, Tibshirani R, Mitchell JD, Richardson D, O'Byrne KJ, Koong AC, Giaccia AJ. An evaluation of tumor oxygenation and gene expression in patients with early stage non-small cell lung cancers. Clin Cancer Res. 2006; 12:1507–1514. [PubMed: 16533775]
20. Vaupel P, Mayer A. Hypoxia in cancer: significance and impact on clinical outcome. Cancer Metast Rev. 2007; 26:225–239.
21. Glowa C, Karger CP, Brons S, Zhao D, Mason RP, Huber PE, Debus J, Peschke P. Carbon ion radiotherapy decreases the impact of tumor heterogeneity on radiation response in experimental prostate tumors. Cancer Letters. 2016; 378:97–103. [PubMed: 27224892]
22. Kodibagkar VD, Wang X, Pacheco-Torres J, Gulaka P, Mason RP. Proton Imaging of Siloxanes to map Tissue Oxygenation Levels (PISTOL): a tool for quantitative tissue oximetry. NMRBiomed. 2008; 21:899–907.
23. Khan N, Mupparaju S, Hekmatyar SK, Hou HG, Lariviere JP, Demidenko E, Gladstone DJ, Kauppinen RA, Swartz HM. Effect of hyperoxygenation on tissue pO_2 and its effect on radiotherapeutic efficacy of orthotopic F98 gliomas. Int J Radiat Oncol Biol Phys. 2010; 78:1193–1200. [PubMed: 20813466]
24. Hou H, Lariviere JP, Demidenko E, Gladstone D, Swartz H, Khan N. Repeated tumor pO2 measurements by multi-site EPR oximetry as a prognostic marker for enhanced therapeutic efficacy of fractionated radiotherapy. Radiother Oncol. 2009; 91:126–131. [PubMed: 19013657]
25. Zhou H, Hallac RR, Lopez RR, Denney R, MacDonough MT, Li LL, Graves LEE, Trawick ML, Pinney KG, Mason RP. Evaluation of tumor ischemia in response to an indole-based vascular disrupting agent using BLI and 19F MRI. Am J Nucl Med Mol Imaging. 2015; 5:143–153. [PubMed: 25973335]
26. Mason RP, Antich PP, Babcock EE, Constantinescu A, Peschke P, Hahn EW. Non-invasive determination of tumor oxygen tension and local variation with growth. Int J Radiat Oncol Biol Phys. 1994; 29:95–103. [PubMed: 8175452]
27. Graves EE, Vilalta M, Cecic IK, Erler JT, Tran PT, Felsher D, Sayles L, Sweet-Cordero A, Le QT, Giaccia AJ. Hypoxia in Models of Lung Cancer: Implications for Targeted Therapeutics. Clin Cancer Res. 2010; 16:4843–4852. [PubMed: 20858837]
28. Baker LCJ, Boult JKR, Jamin Y, Gilmour LD, Walker-Samuel S, Burrell JS, Ashcroft M, Howe FA, Griffiths JR, Raleigh JA, van der Kogel AJ, Robinson SP. Evaluation and Immunohistochemical Qualification of Carbogen-Induced R_2* as a Noninvasive Imaging Biomarker of Improved Tumor Oxygenation. Int J Radiat Oncol Biol Phys. 2013; 87:160–167. [PubMed: 23849692]
29. De Los Santos J, Popple R, Agazaryan N, Bayouth JE, Bissonnette J-P, Bucci MK, Dieterich S, Dong L, Forster KM, Indelicato D, Langen K, Lehmann J, Mayr N, Parsai I, Salter W, Tomblyn M, Yuh WTC, Chetty IJ. Image Guided Radiation Therapy (IGRT) Technologies for Radiation Therapy Localization and Delivery. Int J Radiat Oncol Biol Phys. 2013; 87:33–45. [PubMed: 23664076]
30. Howe FA, Robinson SP, McIntyre DJO, Stubbs M, Griffiths JR. Issues in flow and oxygenation dependent contrast (FLOOD) imaging of tumours. NMR Biomed. 2001; 14:497–506. [PubMed: 11746943]
31. Matsumoto K, Bernardo M, Subramanian S, Choyke P, Mitchell JB, Krishna MC, Lizak MJ. MR assessment of changes of tumor in response to hyperbaric oxygen treatment. Magn Reson Med. 2006; 56:240–246. [PubMed: 16795082]
32. Burrell JS, Walker-Samuel S, Baker LCJ, Boult JKR, Jamin Y, Halliday J, Waterton JC, Robinson SP. Exploring ΔR_2* and ΔR_1 as imaging biomarkers of tumor oxygenation. J Magn Reson Imaging. 2013; 38:429–434. [PubMed: 23293077]
33. Hallac RR, Zhou H, Pidikiti R, Song K, Stojadinovic S, Zhao D, Solberg T, Peschke P, Mason RP. Correlations of noninvasive BOLD and TOLD MRI with pO_2 and relevance to tumor radiation response. Magn Reson Med. 2014; 71:1863–1873. [PubMed: 23813468]
34. Zhao D, Pacheco-Torres J, Hallac RR, White D, Peschke P, Cerdán S, Mason RP. Dynamic oxygen challenge evaluated by NMR T_1 and T_2* – insights into tumor oxygenation. NMR Biomed. 2015; 28:937–947. [PubMed: 26058575]

35. Winter JD, Akens MK, Cheng H-LM. Quantitative MRI assessment of VX2 tumour oxygenation changes in response to hyperoxia and hypercapnia. Phys Med Biol. 2011; 56:1225. [PubMed: 21285489]
36. O'Connor JPB, Naish JH, Jackson A, Waterton JC, Watson Y, Cheung S, Buckley DL, McGrath DM, Buonaccorsi GA, Mills SJ, Roberts C, Jayson GC, Parker GJM. Comparison of Normal Tissue R-1 and R-2* Modulation by Oxygen and Carbogen. Magn Reson Med. 2009; 61:75–83. [PubMed: 19097212]
37. Ding Y, Mason RP, McColl RW, Yuan Q, Hallac RR, Sims RD, Weatherall PT. Simultaneous measurement of tissue oxygen level-dependent (TOLD) and blood oxygenation level-dependent (BOLD) effects in abdominal tissue oxygenation level studies. J Magn Reson Imaging. 2013; 38:1230–1236. [PubMed: 23749420]
38. Remmele S, Sprinkart AM, Muller A, Traber F, von Lehe M, Gieseke J, Flacke S, Willinek WA, Schild HH, Senegas J, Keupp J, Murtz P. Dynamic and simultaneous MR measurement of R1 and R2*changes during respiratory challenges for the assessment of blood and tissue oxygenation. Magn Reson Med. 2013; 70:136–146. [PubMed: 22926895]
39. Al-Hallaq HA, River JN, Zamora M, Oikawa H, Karczmar GS. Correlation of magnetic resonance and oxygen microelectrode measurements of carbogen-induced changes in tumor oxygenation. Int J Radiat Oncol Biol Phys. 1998; 41:151–159. [PubMed: 9588930]
40. Baudelet C, Gallez B. How does blood oxygen level-dependent (BOLD) contrast correlate with oxygen partial pressure (pO_2) inside tumors? Magn Reson Med. 2002; 48:980–986. [PubMed: 12465107]
41. Zhao D, Jiang L, Hahn EW, Mason RP. Comparison of ^{1}H blood oxygen level-dependent (BOLD) and ^{19}F MRI to investigate tumor oxygenation. Magn Reson Med. 2009; 62:357–364. [PubMed: 19526495]
42. Timmerman R, Paulus R, Galvin J, Michalski J, Straube W, Bradley J, Fakiris A, Bezjak A, Videtic G, Johnstone D, Fowler J, Gore E, Choy H. Stereotactic Body Radiation Therapy for Inoperable Early Stage Lung Cancer. JAMA. 2010; 303:1070–1076. [PubMed: 20233825]
43. Carlson DJ, Keall PJ, Loo BW, Chen ZJ, Brown JM. Hypofractionation Results in Reduced Tumor Cell Kill Compared to Conventional Fractionation for Tumors with Regions of Hypoxia. Int J Radiat Oncol Biol Phys. 2011; 79:1188–1195. [PubMed: 21183291]
44. Isaacs J, Heston W, Weissman R, Coffey D. Animal models of the hormone sensitive and insensitive prostatic adenocarcinomas, Dunning R3327-H, -HI and AT. Cancer Res. 1978; 38:4353–4359. [PubMed: 698976]
45. Peschke P, Hahn EW, Wenz F, Lohr F, Braunschweig F, Wolber G, Zuna I, Wannenmacher M. Differential Sensitivity of Three Sublines of the Rat Dunning Prostate Tumor System R3327 to Radiation and/or Local Tumor Hyperthermia. Radiat Res. 1998; 150:423–430. [PubMed: 9768856]
46. Karger CP, Peschke P, Scholz M, Huber PE, Debus J. Relative Biological Effectiveness of Carbon Ions in a Rat Prostate Carcinoma In Vivo: Comparison of 1, 2, and 6 Fractions. Int J Radiat Oncol Biol Phys. 2013; 86:450–455. [PubMed: 23474116]
47. Ljungkvist ASE, Bussink J, Kaanders J, Van der Kogel AJ. Dynamics of tumor hypoxia measured with bioreductive hypoxic cell markers. Radiat Res. 2007; 167:127–145. [PubMed: 17390721]
48. Rodrigues LM, Howe FA, Griffiths JR, Robinson SP. Tumor R-2 * is a prognostic indicator of acute radiotherapeutic response in rodent tumors. J Magn Reson Imaging. 2004; 19:482–488. [PubMed: 15065173]
49. O'Connor JPB, Naish JH, Parker GJM, Waterton JC, Watson Y, Jayson GC, Buonaccorsi GA, Cheung S, Buckley DL, McGrath DM, West CML, Davidson SE, Roberts C, Mills SJ, Mitchell CL, Hope L, Ton C, Jackson A. Preliminary Study of Oxygen-Enhanced Longitudinal Relaxation in MRI: a Potential Novel Biomarker of Oxygenation Changes in Solid Tumors. Int J Radiat Oncol Biol Phys. 2009; 75:1209–1215. [PubMed: 19327904]
50. Mason RP, Hunjan S, Le D, Constantinescu C, Barker BR, Wong PS, Peschke P, Hahn EW, Antich PP. Regional Tumor Oxygen Tension: Fluorine Echo Planar Imaging of Hexafluorobenzene Reveals Heterogeneity of Dynamics. Int J Radiat Oncol Biol Phys. 1998; 42:747–750. [PubMed: 9845089]

51. Timmerman R, Paulus R, Galvin J, et al. Stereotactic body radiation therapy for inoperable early stage lung cancer. JAMA. 2010; 303:1070–1076. [PubMed: 20233825]
52. Beeman SC, Shui Y-B, Perez-Torres CJ, Engelbach JA, Ackerman JJH, Garbow JR. O_2-sensitive MRI distinguishes brain tumor versus radiation necrosis in murine models. Magn Reson Med. 2015; 75:2442–2447. [PubMed: 26175346]
53. Lin Y-C, Wang J-J, Hong J-H, Lin Y-P, Lee C-C, Wai Y-Y, Ng S-H, Wu Y-M, Wang C-C. Noninvasive Monitoring of Microvascular Changes With Partial Irradiation Using Dynamic Contrast-Enhanced and Blood Oxygen Level-Dependent Magnetic Resonance Imaging. Int J Radiat Oncol Biol Phys. 2013; 85:1367–1374. [PubMed: 23195777]
54. Leonard KL, Logan JK, Dermarkar P, Patel S, Wazer DE, DiPetrillo TA. Effect of Modern Radiation Therapy Techniques on Hematocrit in Patients With Prostate Cancer. Int J Radiat Oncol Biol Phys. 2013; 87:S344.
55. Song CW, Lee YJ, Griffin RJ, Park I, Koonce NA, Hui S, Kim MS, Dusenbery KE, Sperduto PW, Cho LC. Indirect Tumor Cell Death After High-Dose Hypofractionated Irradiation: Implications for Stereotactic Body Radiation Therapy and Stereotactic Radiation Surgery. Int J Radiat Oncol Biol Phys. 2015; 93:166–172. [PubMed: 26279032]
56. Jiang L, Weatherall PT, McColl RW, Tripathy D, Mason RP. Blood oxygenation level-dependent (BOLD) contrast magnetic resonance imaging (MRI) for prediction of breast cancer chemotherapy response: A pilot study. J Magn Reson Imaging. 2013; 37:1083–1092. [PubMed: 23124705]
57. Rakow-Penner R, Daniel B, Glover GH. Detecting Blood Oxygen Level-Dependent (BOLD) Contrast in the Breast. J Magn Reson Imaging. 2010; 32:120–129. [PubMed: 20578018]
58. Hallac RR, Ding Y, Yuan Q, McColl RW, Lea J, Sims RD, Weatherall PT, Mason RP. Oxygenation in cervical cancer and normal uterine cervix assessed using blood oxygenation level-dependent (BOLD) MRI at 3T. NMR Biomed. 2012; 25:1321–1330. [PubMed: 22619091]
59. Li XS, Fan HX, Fang H, Song YL, Zhou CW. Value of R2* obtained from T2*-weighted imaging in predicting the prognosis of advanced cervical squamous carcinoma treated with concurrent chemoradiotherapy. Journal of Magnetic Resonance Imaging. 2015; 42:681–688. [PubMed: 25581675]
60. Linnik IV, Scott MLJ, Holliday KF, Woodhouse N, Waterton JC, O'Connor JPB, Barjat H, Liess C, Ulloa J, Young H, Dive C, Hodgkinson CL, Ward T, Roberts D, Mills SJ, Thompson G, Buonaccorsi GA, Cheung S, Jackson A, Naish JH, Parker GJM. Noninvasive tumor hypoxia measurement using magnetic resonance imaging in murine U87 glioma xenografts and in patients with glioblastoma. Magn Reson Med. 2014; 71:1854–1862. [PubMed: 23798369]
61. Alonzi R, Padhani AR, Maxwell RJ, Taylor NJ, Stirling JJ, Wilson JI, d'Arcy JA, Collins DJ, Saunders MI, Hoskin PJ. Carbogen breathing increases prostate cancer oxygenation: a translational MRI study in murine xenografts and humans. Br J Cancer. 2009; 100:644–648. [PubMed: 19190629]
62. Patterson AJ, Priest AN, Bowden DJ, Wallace TE, Patterson I, Graves MJ, Lomas DJ. Quantitative BOLD imaging at 3T: Temporal changes in hepatocellular carcinoma and fibrosis following oxygen challenge. Journal of Magnetic Resonance Imaging. 2016 n/a-n/a.

Highlights

- Hypoxia is associated with radiation resistance, particularly for SBRT.
- Non-invasive OE-MRI is a potential biomarker to predict tumor response.
- Breathing oxygen enhanced radiation response, with a wide range of responses.
- OE-MRI demonstrates a correlation between T_1-weighted contrast and radiation response.
- OE-MRI is highly translational.

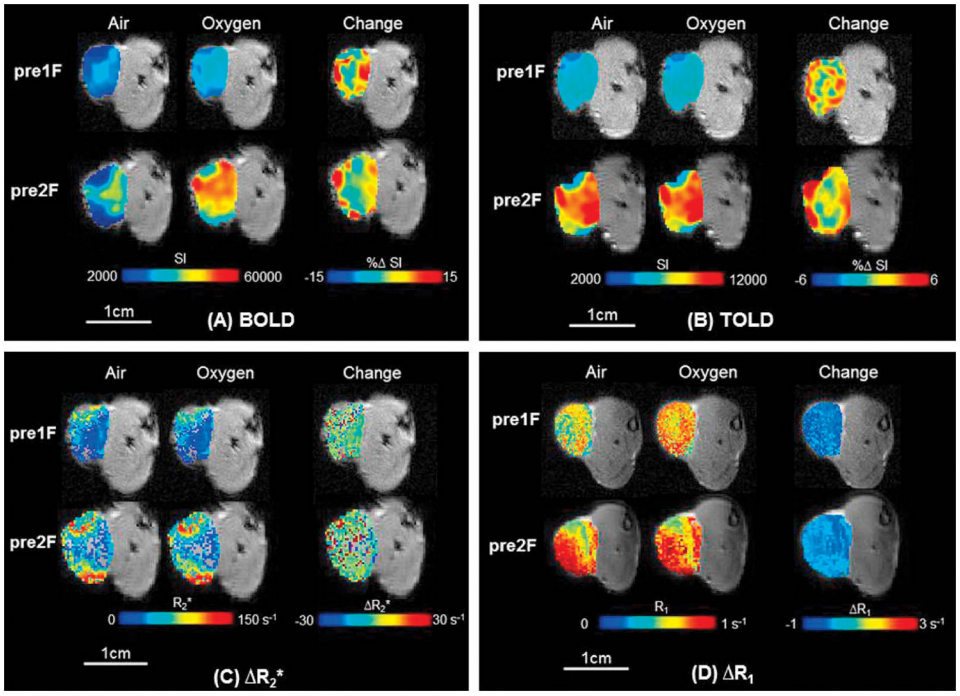

Figure 1. Oxygen-Enhanced MRI

Response maps overlaid on transaxial MR images of representative subcutaneous R3327-AT1 tumor (0.9 cm^3; #3) in rat thigh. Heterogeneity of baseline values and response to oxygen breathing is apparent. There was minimal change in tumor volume over one week following 15 Gy irradiation while breathing oxygen.

A) Upper-Left panel: BOLD maps overlaid on T_2*-weighted images. Top row: Before the first irradiation. Mean baseline T_2*-weighted signal intensity maps are shown for air breathing (left) and oxygen breathing (center), together with the response map with respect to inhaling oxygen for 2 minutes (right; %ΔSI). The greatest increase in signal appears around the tumor periphery, which is generally better vascularized. Bottom row: Corresponding maps one week later.

B) Upper-Right panel: Corresponding TOLD maps overlaid on T_1-weighted images. Top row: Before the first irradiation. Mean baseline T_1-weighted signal intensity maps are shown for air breathing (left) and oxygen breathing (center) together with the response map with respect to inhaling oxygen for 2 minutes (right; %ΔSI). Again the greatest increase in signal appears around the tumor periphery. Bottom row: Corresponding maps one week later.

C) Lower-Left panel: Quantitative R_2* maps. Top row: left) Baseline breathing air (mean R_2*=38±25 s^{-1}), middle) breathing oxygen (mean R_2*=37±23 s^{-1}), and right) ΔR_2* (mean =−1±34 s^{-1}) response before the first irradiation. Bottom row: Corresponding maps one week later: left) air (mean R_2* = 64.4±1.6 s^{-1}); middle) oxygen (mean R_2* = 64.7±1.7 s^{-1}); and right) ΔR_2* (mean = 0.3±2.3 s^{-1}) response before the second irradiation.

D) Lower-Right panel: Quantitative R_1 maps. Top row: left) Baseline breathing air (mean R_1 = 0.68±0.16 s^{-1}), center) breathing oxygen (mean R_1=0.75±0.14 s^{-1}); and right) ΔR_1 (mean =0.07±0.29 s^{-1}) response before the first irradiation. Bottom row: Corresponding maps one week later: left) air (mean R_1 = 0.6295±0.0040 s^{-1}); center) oxygen (mean R_1 =

0.607±0.004 s^{-1}); and right) ΔR_1 (mean = 0.0015±0.0059 s^{-1}) response before the second irradiation.

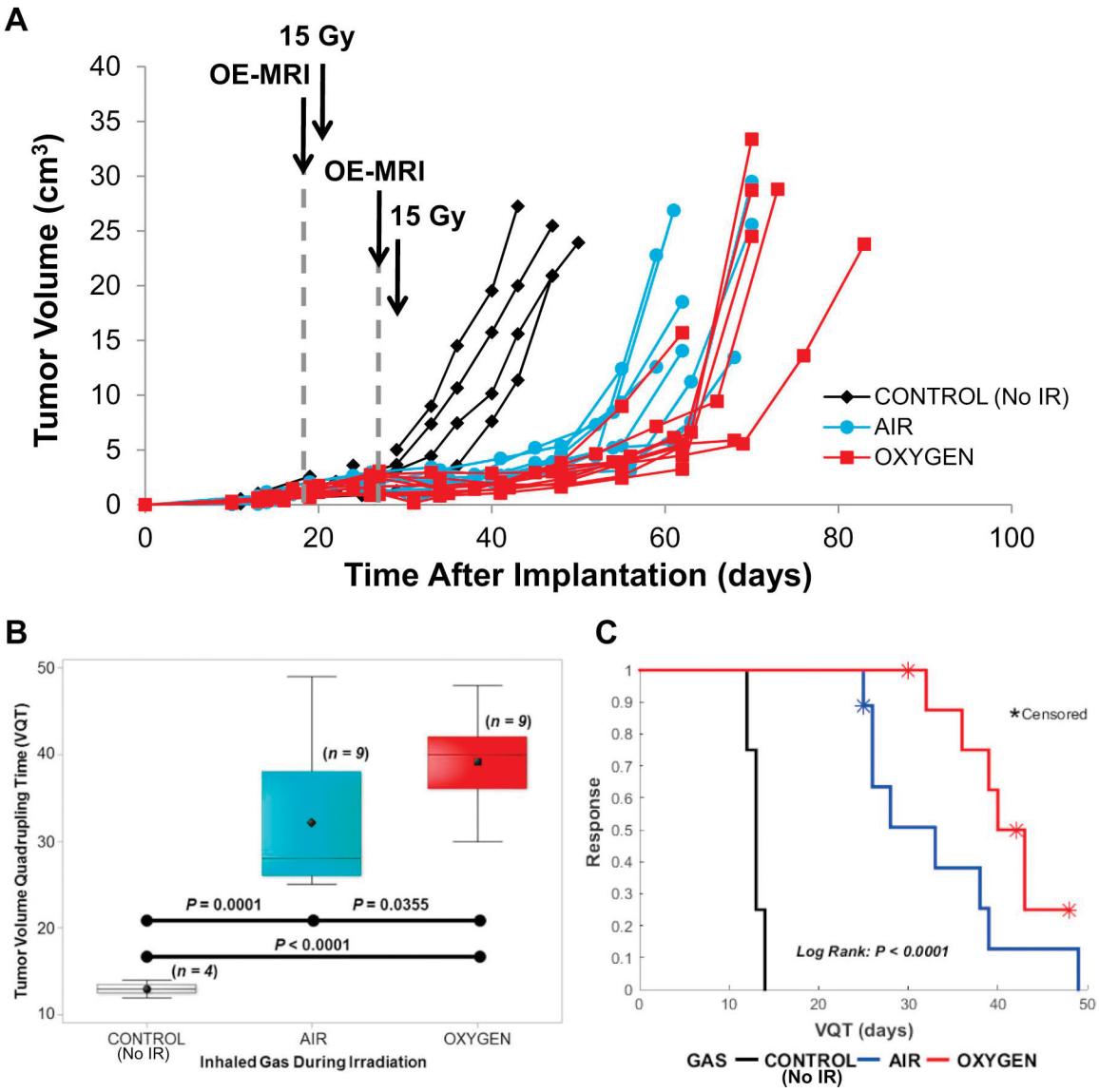

Figure 2. Tumor response to radiation

A) Growth curves for individual Dunning prostate R3327-AT1 tumors: non-irradiated control tumors (Group 1; $n = 4$, black diamonds), irradiated while breathing Air (Group 2; $n = 9$, blue circles), or irradiated while breathing Oxygen (Group 3; $n = 9$, red squares). Irradiated tumors showed an obvious growth delay in response to a split-dose schedule of 2F × 7.5 Gy AP/PA 7 days apart.

B) Irradiation caused a significant tumor growth delay as shown for time to quadruple in volume (VQT). Tumors on rats breathing oxygen showed a significantly greater delay. Box and whiskers plots show mean, median, inter quartile and full ranges.

C) The tumor growth delay is apparent in the Kaplan-Meier survival plot. The log rank test (adjusted for five (1 air and 4 oxygen) censored indicated significant differences among the irradiation breathing treatment event time distributions.

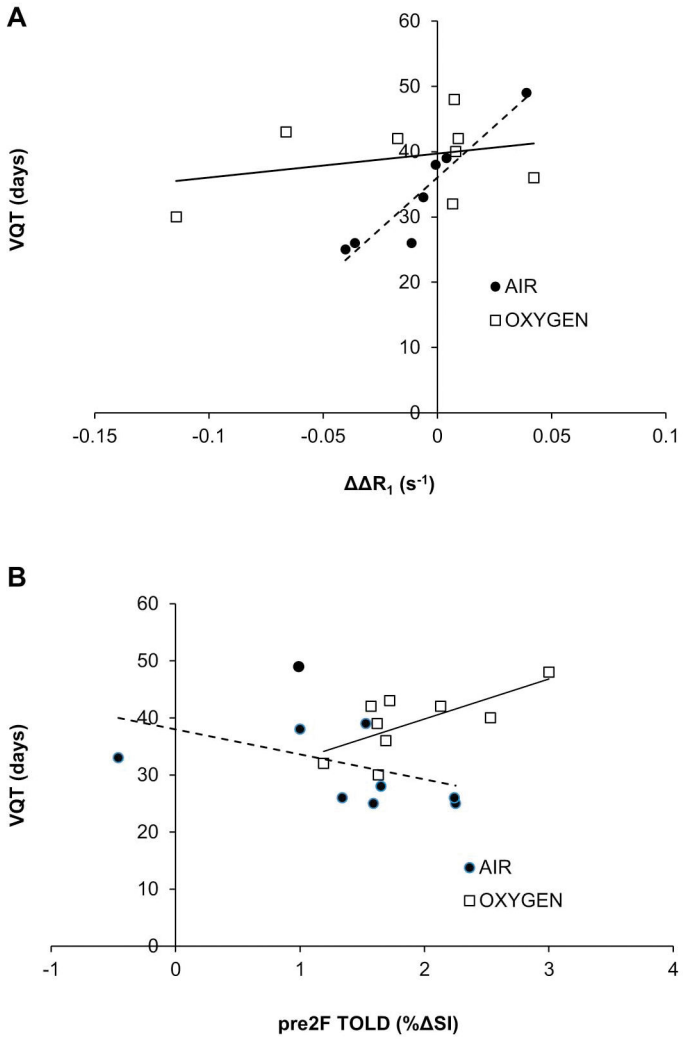

Figure 3. Correlations between OE-MRI and tumor growth delay

Data separated with respect to inhaled gas during tumor radiation: Air (filled circles) or Oxygen, (open squares) versus time to reach four times the initial irradiated tumor volume (VQT). A) Strong correlation was observed for the difference in responses between the 2nd and 1st ΔR_1 ($\Delta\Delta R_1$) and VQT (R >0.93, P <0.002) for those animals inhaling Air, but much weaker for the Oxygen Group. B) A moderate correlation was observed between TOLD before the 2nd irradiation and VQT (R >0.6, P =0.0051) for animals breathing Oxygen, but not Air.

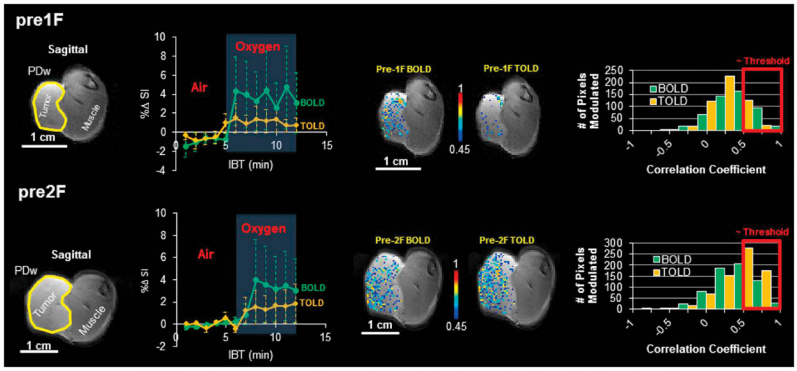

Figure 4. Evidence for tumor reoxygenation

Response to oxygen breathing challenge may be assessed as mean signal response, but data may be compromised by noise. Correlation coefficient mapping identifies response more robustly. Top row prior to first irradiation. Left- proton density image of AT1 tumor #6 (1.4 cm^3). Center left) dynamic BOLD and TOLD mean %ΔSI measurements obtained interleaved with respect to oxygen breathing challenge; Right) corresponding voxel-by-voxel correlation coefficient maps and histograms before each dose fraction. BOLD and TOLD histograms appear to be normally distributed below the threshold (0.45). At the threshold, the histograms show modest response.

Bottom row. Corresponding data one week later before the 2nd irradiation indicate some tumor growth, but similar mean BOLD and TOLD response. However, the number of responsive voxels selected with a 0.45 correlation coefficient thresholds now much greater and corresponding histograms are skewed revealing a larger proportion of voxels modulated by oxygen breathing challenge after irradiation

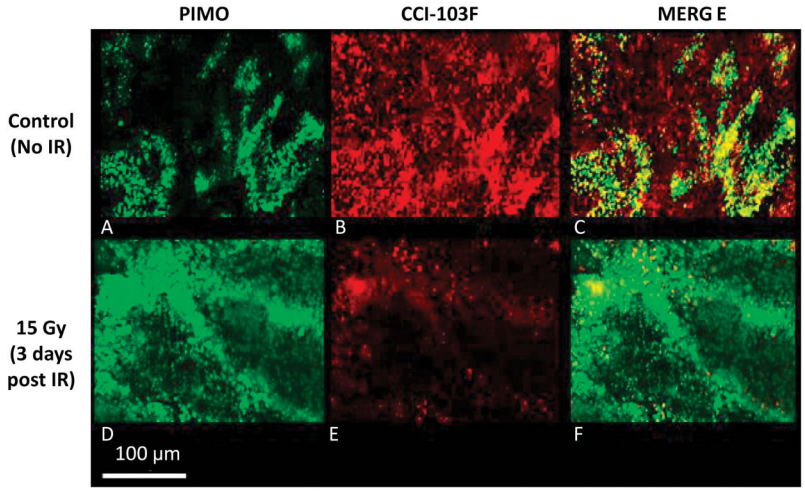

Figure 5. Immunohistochemical validation of reoxygenation

Non-irradiated tumor (control, top row) and a tumor irradiated while breathing oxygen (bottom row). Pimonidazole (green A, D) and CCI-103F (red B, E) hypoxia markers showed consistent extensive retained hypoxia in control tumor (overlap appears yellow C, F). The irradiated tumor showed much less hypoxia three days after 15 Gy, consistent with reoxygenation and the increase in the number of modulated BOLD and TOLD voxels seen in Fig. 4. Both hypoxia markers were administered while rats breathed oxygen on each occasion. (Original magnification 20X)

Table 1

Chronological Scheme of Measurements and Irradiation

Day	0	19	19	20	23	26	27	Termination
Procedure	Implant	OE-MRI *	Pimonidazole	IR 15 Gy	CCI-103F	OE-MRI	IR 15 Gy	VQT, 10%BW loss 90 days
Group 1 No IR	n=4							✓
Group 2 2×15 Gy Air	n=9	Air → O_2 R_1, IBT, R_1		Air		Air → O_2 R_1, IBT, R_1	Air	✓
Group 3 2×15 Gy O_2	n=9	Air → O_2 R_1, IBT, R_1		O_2		Air → O_2 R_1, IBT, R_1	O_2	✓
Group 4 IHC	n=3	Air → O_2 R_1, IBT, R_1	O_2	O_2 (n=2)	OE-MRI, O_2, sacrifice			

R_1, IBT, R_1 indicates baseline R_1 map followed by interleaved R_2 maps and T_1-weighted images during transition to oxygen followed by final R_1 map with O_2 breathing.

Table 2

Dunning R3327-AT1 Prostate Tumor Characteristics and Results for Hypofractionation

AT1 Tumor	Tumor Size (cm^3)		BOLD (%ΔSI)		TOLD (%ΔSI)		ΔR_1 (s^{-1})		ΔR_2* (s^{-1})			
	pre1F	pre2F	pre1F	pre2F	pre1F	pre2F	pre1F	pre2F	pre1F	pre2F	VQT (days)	VDT (days)
1	1.0	2.7	−2.10±0.54	2.36±0.76	−0.40±0.21	2.25±0.58	0.0539±0.0010	ND	5.1±1.7	1.3±1.0	19	25
2	0.9	1.6	3.62±0.29	2.59±0.33	2.13±0.25	1.65±0.20	0.0475±0.0017	ND	0.3±1.8	−1.7±1.0	18	28
3	0.9	1.2	−0.60±0.47	5.18±0.53	−0.19±0.15	1.34±0.79	0.0928±0.0017	0.0567±0.0011	−3.5±2.4	2.6±1.7	21	26
4	1.2	2.3	4.09±1.59	−0.33±0.33	2.51±0.24	−0.46±0.09	0.0374±0.0013	0.0313±0.0008	−0.8±2.3	0.9±1.6	17	33
5	1.2	2.5	2.43±0.56	1.86±0.34	0.79±0.04	1.00±0.17	0.0149±0.0013	0.0142±0.0011	9.1±1.6	−0.1±1.0	7	28
6	1.4	2.2	4.01±0.33	3.01±0.46	1.05±0.34	1.53±0.15	0.0099±0.0023	0.0139±0.0015	−0.3±2.1	−0.1±2.7	23	39
7	2.1	3.1	−0.44±0.26	0.73±0.17	0.59±0.11	0.98±0.17	−0.006±0.0008	0.0326±0.0008	−0.4±0.8	−0.3±0.5	31	49
8	0.9	1.0	3.76±0.63	3.86±0.87	2.11±0.30	2.24±0.32	0.0365±0.0006	0.0252±0.0151	0.6±2.1	0.6±1.6	13	26
9	1.2	2.0	3.29±0.46	2.28±0.27	0.72±0.57	1.59±0.40	0.0472±0.0023	0.0070±0.0031	−0.6±0.9	0.3±1.2	10	25
Inhaled Air Mean±SEM	**1.2±0.1**	**2.0±0.2**	**2.0±0.8**	**2.4±0.5**	**1.0±0.3**	**1.35±0.27**	**0.0371±0.0100**	**0.026±0.006**	**1.1±1.3**	**0.4±0.4**	**18±2**	**32±3**
10	1.5	1.7	−0.93±0.55	2.52±0.59	0.32±0.16	1.62±0.29	0.0460±0.0018	ND	−1.0±1.7	−3.2±1.1	28	39
11	1.1	1.7	−3.26±0.62	3.29±0.62	1.07±0.14	1.63±0.19	0.1213±0.0023	0.0070±0.0018	2.1±1.6	−0.3±1.1	24	30
12	0.7	1.1	1.43±0.20	0.61±0.40	0.76±0.12	1.19±0.17	0.0393±0.0018	0.0460±0.0013	1.7±2.4	1.0±1.8	23	32
13	0.9	0.9	4.52±0.95	4.77±0.64	1.97±0.19	1.72±0.24	0.0677±0.0014	0.0015±0.0022	−1.0±1.3	0.3±2.3	31	43
14	1.2	2.5	3.55±1.29	3.24±0.45	0.77±0.26	2.53±0.22	0.0520±0.0021	0.0601±0.0036	−1.5±1.8	−0.3±1.0	25	40
15	1.1	0.9	7.94±0.80	2.22±0.47	1.40±0.33	1.68±0.20	0.0308±0.0017	0.0730±0.0013	−3.3±1.3	−2.4±1.6	28	36
16	1.6	2.7	1.64±0.27	2.50±0.44	1.25±0.15	1.57±0.15	0.0310±0.0011	0.0136±0.0013	−0.8±1.2	−2.3±0.8	30	42
17	1.7	2.6	2.60±0.60	3.43±0.57	1.03±0.23	3.00±0.56	0.0011±0.0016	0.0085±0.0008	5.4±1.4	−3.3±0.9	28	48
18	1.7	3.1	4.77±0.64	3.47±0.51	1.51±0.14	2.13±0.20	0.0069±0.0010	0.0161±0.0009	−1.2±1.1	−0.5±1.1	37	42
Inhaled Oxygen Mean±SEM	**1.3±0.1**	**1.9±0.3**	**2.5±1.1**	**2.9±0.4**	**1.1±0.2**	**1.9±0.2**	**0.044±0.012**	**0.028±0.010**	**0.04±0.86**	**−1.2±0.5**	**28±1**	**39±2**
Overall Mean±SEM	1.3±0.1	2.1±0.2	2.2±0.7	2.6±0.3	1.1±0.2	1.6±0.2	0.041±0.007	0.027±0.006	0.55±0.75	−0.42±0.38	20±2	32±2
P-value[a]	0.7093[a]	0.7160[a]	0.7351[a]	0.4576[a]	0.8241[a]	0.1144[a]	0.6570[a]	0.8449[a]	0.5155[a]	**0.0271**[a]	**0.0006**[a]	**0.0356**[a]
P-value[b,c]	0.4235[b], 0.5799 [c]		0.9822[b]		0.4242[b]		0.7071[b]		0.7353[b]		**<0.0001** [c]	**<0.0001** [c]

Data values reported as mean ± standard error of the mean (SEM) from voxels averaged over two slices for BOLD, TOLD, and R_2* and three slices for R_1.

ND- missing values due to logistic issues.

[a] – *P*-values for comparisons (two-sample *t*-tests) of each covariate for differences in inhaling air vs. oxygen.

[b] – *P*-values for comparisons (two-sample *t*-tests) of each covariate for differences in pre1F- vs. pre2F controlled treatment groups (inhaling air vs. oxygen)

[c] – *P*-values for comparisons (general linear analysis) in differences of initial, VDT, or VQT tumor volumes vs. control tumor volumes (not shown in table).

VDT: time the tumors reached 2 times the initial irradiated tumor volume; VQT: time the tumors reached 4 times the initial irradiated tumor volume

BOLD: blood-oxygenation level dependent; TOLD: tissue-oxygenation level dependent; ΔR_1: intrinsic longitudinal relaxation rate; ΔR_2^*: apparent transverse relaxation rate

pre1F- measurements before the first irradiation

pre2F- measurements six days after the first irradiation and before the second irradiation

Cancer Lett. Author manuscript; available in PMC 2017 September 28.